A Hidden Markov Model for Distinguishing between RFID-tagged Objects in Adjacent Areas

Matthias Hauser, Matthias Griebel and Frédéric Thiesse
Chair of Information Systems Engineering
University of Würzburg, Germany
Email: {matthias.hauser, matthias.griebel, frederic.thiesse}@uni-wuerzburg.de

***Abstract*—Distinguishing between RFID-tagged objects within different areas poses an important building block for many RFID-based applications. Existing localization techniques, however, often cannot reliably distinguish between tagged objects that are close to the border of adjacent areas. Against this backdrop, we present a hybrid approach based on an ANN and a HMM that leverages not only low-level RFID data streams but also information about physical constraints and process knowledge and thus incorporates scene dynamics. We experimentally demonstrate the performance of our approach considering a RFID-based *smart* fitting room which is a practically relevant application with limited process control in an environment with strong multipath reflections and non-line-of-sight effects. Our results show that our approach is able to reliably distinguish between tagged objects within different cabins. This includes objects hanging on coat hooks at partition walls of adjacent cabins, i.e., at a maximum distance of 5 centimeters to the border of an adjacent area.**

I. Introduction

Techniques for indoor localization of RFID-tagged objects have attracted considerable attention in recent years and pose an important building block for many existing and forthcoming RFID-based applications [1], [2]. The prediction of physical coordinates is, however, often not necessary [3], [4]. Instead, many applications depend on the ability of a localization system (i) to reliably distinguish between RFID-tagged objects within adjacent areas and (ii) to timely detect transitions between these areas. Such RFID-based systems are, e.g., gates in stores that detect transitions between sales floor and backroom as well as article surveillance or automated checkout systems that detect items carried out of a store.

The major techniques used for RFID indoor localization are (i) triangulation, (ii) proximity, and (iii) scene analysis [2]. The first technique uses distance measurements between reference points, the second relies on the measurement of the nearness of a set of neighboring points with known positions. The third technique consists of an offline (or training) and an online (or run time) phase. The objective within the offline phase is to analyze relationships between signal strength measurements and positions within a particular scene (usually the environment where the localization system is deployed). Then, during the online phase locations of RFID-tagged objects are estimated based on the previously collected data.

While many authors (e.g., [5]–[7]) compare new measurements to the closest a priori measurement in a database (offline phase), more sophisticated pattern recognition techniques may be applied as well. Prominent examples are support vector machines and artificial neural networks (ANN). Both models allow the formulation of the localization problem as a regression and as a classification problem [8]. In the first case, physical coordinates of tagged-objects are learned during the offline phase and estimated during the online phase. The formulation of the classification problem, on the other hand, requires dividing the scene into selected areas. During the offline phase the machine learning model learns the radio signal behavior within these areas. Then, during the subsequent online phase, the RFID raw data streams of tagged objects are matched to areas with closest radio signal characteristics.

In this paper, we apply a scene-based algorithm based on an ANN classification model to learn RFID signal behavior within selected areas. During the online phase, the output vector of the model at a given time represents an estimate of being within a specific area. In contrast to previous literature, we do not directly translate these estimates into the most probable area, i.e., the area with the highest probability. Instead, we feed the probabilities into a hidden Markov model (HMM). This model is designed based on information about physical constraints (e.g., layout of walls) and process knowledge and thus incorporates the dynamics of the scene. By leveraging this additional information, we enable our system to reliably distinguish between RFID-tagged objects in selected areas, including those that are close to the borders of adjacent ones.

We experimentally demonstrate the performance of our approach considering an RFID-based *smart* fitting room. This application represents a practically relevant application on the retail sales floor that detects garments within cabins and offers additional services such as information on garments (e.g., available colors or sizes) or product recommendations [9]. We intentionally choose an application in an environment with strong multipath reflections (e.g., ceiling, floor, customers) and non-line-of-sight effects which are very challenging for RFID tag localization [10]–[12]. In contrast to applications in the upstream retail supply chain (e.g., conveyor belts or gates in distribution centers), *smart* fitting rooms furthermore represent an application with limited process control. This is because every customer behaves differently (e.g., different movement speed and movement paths) and firms can not

978-1-5090-4576-1/17/$31.00 ©2017 IEEE

978-1-5090-4576-1/17/$31.00 ©2017 IEEE

instruct them how to deal with the technology (in contrast to their own employees in the distribution center).

II. Related Work

Several authors have investigated combining data from sensor streams with additional information to improve indoor localization for applications with limited process control within environments with strong multipath reflections and non-line-of-sight effects.

The user location and tracking system RADAR, for instance, uses information about its environment for the development of an accurate signal propagation model [13]. The authors use building floor information to calculate floor attenuation factor propagation and wall attenuation factor propagation models to compensate for the effects of floors and walls on radio wave propagation between receivers and transmitters. In a later study [14], the system is enhanced with an algorithm that calculates shortest paths of users to determine their most likely trajectory. The objective is to leverage temporal correlations in the data or, as the authors put it, "to use information from the past to come up with a better guess of a user's location" [14]. In doing so, the system considers physical constraints and thus prevents from predictions where users randomly jump about over large distances. Similarly, our RFID-based system combines information about physical constraints with low-level sensor data.

On the other hand, some systems presented in the literature combine HMMs with RF data and information from additional sensors. Goller et al. [11], for example, fuse RFID data with a computer vision system to track and follow tagged objects. We decided against using camera systems because many applications exist where we expect that people have reservations against them (e.g., fitting rooms). Apart from this, Seitz et al. [6], Huang et al. [5], and Yuanfeng et al. [7], present HMM based approaches that combine a phone's inertial sensors (e.g., accelerometers, magnetometers, and gyroscopes) with WiFi data to track and follow a person's mobile phone.

III. Approach

Our HMM based approach fuses information from existing RFID systems with information about physical constraints and process knowledge. It combines state-of-the-art machine learning with probabilistic modelling and enables us to reliably and timely detect locations of tagged objects. In the following subsections, we shortly introduce HMMs, describe the connection of the ANN output to the HMM, and present an *adjusted* Viterbi algorithm that decodes the location of tagged objects in real-time.

A. Hidden Markov Models

HMMs are statistical models situated in partially observable environments which means that the actual locations of RFID tags can not be observed directly. HMMs are built up from a finite set of N distinct *hidden* states $Q = \{q_1, \ldots, q_N\}$. It is, however, possible to physically observe a sequence $O = \{o_1, \ldots, o_M\}$ where each o_m can be represented by a vector of RFID-signal based features. All states q_n are associated with a probability function $p(o_m|q_n)$[1] of emitting an observation o_m at a given state q_n. Furthermore, we define initial and transition probabilities based on physical constraints and process information. The initial state distribution $\pi = \{\pi_i\}$, on the one hand, represents the probability of starting in a specific state q_i at time $t = 1$. Transition probabilities $A = \{a_{i,j}\}$, on the other hand, define the probabilities of state transitions from q_i to q_j.

B. ANNs as Statistical Estimators for Emission Probabilities

Bourlard and Wellekens [15] propose the use of ANNs as estimators for HMM emission probabilities instead of conventional (gaussian-based) methods. This offers several advantages including the combination of discrete and continuous features as well as the omission of detailed assumptions about the form of the statistical distribution of the real-world observations. Richard and Lippmann [16] proved that ANNs – in this case feed-forward multilayer perceptrons with a *Cross Entropy* cost function – can be trained to produce the *posterior* probability $P(q_n|o_m)$ without losing the mathematical properties of the HMM. Since the proof is based on the minimized criterion (and not on the architecture of the ANN), it is only valid for a sufficiently complex ANN (e.g., it must contain enough parameters) and it must be trained to a global error minimum [17].

As the ANN produces *posterior* probabilities, they must be converted by applying Bayes' rule [18]:

$$\frac{P(q_n|o_m, \theta)}{P(q_n)} = \frac{p(o_m|q_n, \theta)}{p(o_m|\theta)} \tag{1}$$

θ represents the parameter set of the ANN. By dividing the *posterior* estimates $P(q_n|o_m, \theta)$ from the ANN outputs by estimates of the class priors $P(q_n)$, it is possible to compute the estimated scaled emission probability $\frac{P(o_m|q_n,\theta)}{P(o_m|\theta)}$. This may be used as an estimate for the emission probability $p(o_m|q_n)$, since the scaling factor $p(o_m|\theta)$ remains constant for all states[2]. To obtain the prior probabilities $P(q_n)$, training data or specific knowledge about the environment can be used. If there are no strong beliefs about $P(q_t)$, it is common practice to use an uninformative prior that does not change the implication of $P(q_n|o_m, \Theta)$, e.g., a discrete uniform distribution [19].

C. The Adjusted Viterbi Algorithm

Given a HMM λ and the observation sequence $O = \{o_1\ o_2 \ldots o_T\}$, the Viterbi algorithm can be applied to decode the single best state sequence $Q = \{q_1\ q_2 \ldots\ q_T\}$ which in our approach represents the most probable paths of

[1] In this paper, actual probabilities are denoted $P(\cdot)$ while probability density functions are denoted as $p(\cdot)$.

[2] In our approach we map the classes of the ANN classification problem to the corresponding states of the HMM.

tagged items. $\delta_t(i)$ approximates the probability of $P(O|\lambda)$ as the joint probability

$$\delta_t(i) = \max_{q_1,q_2,\ldots,q_{t-1}} P(q_1 \ldots q_t = i,\ o_1 \ldots o_t|\lambda). \quad (2)$$

The *original* Viterbi algorithm [20], [21] then computes the maximum likelihood state sequence using path backtracking which means that it can only be calculated once the whole observation sequence O is available. To solve the localization task in real-time it is, however, necessary to provide information for any o_t immediately. In other words, it must be possible to evaluate the model at any point in time t, even if O is not entirely known. Following the notation of Rabiner [22], our *adjusted* Viterbi algorithm thus computes the most probable path for real-time applications q^r in three steps, dynamically repeating step two and three for $t = 2 \leq t \leq T$:

1) Initialization:

$$\delta_1(i) = \pi_i p(o_1|q_i), \qquad 1 \leq i \leq N \quad (3)$$

2) Recursion:

$$\delta_t(j) = \max_{1\leq i\leq N}[\delta_{t-1}(i)a_{ij}]p(o_t|q_j), \quad \begin{matrix} 2 \leq t \leq T \\ 1 \leq j \leq N \end{matrix} \quad (4)$$

3) Path (state sequence) tracking:

$$q_1^r = \underset{1\leq j\leq N}{\operatorname{argmax}}[\delta_1(j)] \quad (5)$$

$$q_t^r = \underset{1\leq j\leq N}{\operatorname{argmax}}[\delta_t(j)f(a_{q_{t-1}^r j})], \quad 2 \leq t \leq T \quad (6)$$

The function $f(a_{ij})$ is defined as follows:

$$f(a_{ij}) = \begin{cases} 0, & \text{if } a_{ij} = 0 \\ 1, & \text{if } a_{ij} > 0 \end{cases} \quad \forall i, j. \quad (7)$$

Equation 6 prevents the algorithm from performing physically impossible transitions ($a_{ij} = 0$) in case the most probable path would "change" due to the backtracking characteristics of the *original* Viterbi algorithm. Nevertheless, the algorithm approaches the most probable path in the long run as the information stored in δ remains unchanged.

IV. Experiment

We evaluate our approach considering an RFID-based *smart* fitting room application in the laboratory under real-world conditions. In the following subsections, we describe the experimental setup, the collection of the training and test data, the data preparation and the instantiation of the ANN, the modelling of the HMM, and the performance measures. Finally we present the evaluation results.

A. Experimental setup

Our experimental setup with three fitting room cabins and one ceiling-mounted RFID system is depicted in Fig. 1. We use the Impinj xArray gateway which includes a reader device and an antenna array with 52 far-field antenna beams mounted in one housing [23]. The RF frequency changes between the four allowed channels in Europe's ETSI region (865.7, 866.3, 866.9, and 867.5 MHz) [23]. The cabins consist of thin wooden walls which do not shield RFID signals.

Applying a scene-based algorithm to a multiclass classification problem requires dividing the scene into designated areas and collecting training data for each of these areas. As shown in Fig. 1b we divided the setup into 24 grid fields of equal size (0.6m×0.6m). Each fitting room (*Cab1*, *Cab2*, and *Cab3*) comprises four and the area in front of the fitting rooms (*Out1*, *Out2*, and *Out3*) twelve grid fields. We chose the cabin layout and the dimensions according to real-world fitting rooms at one of our industry partners.

To assess the performance of our approach, we additionally installed a light barrier to identify the exact time a tagged garment was moved into one of the cabins. This information is, however, not used by the ANN or the HMM model and the light barrier is thus not needed for our application.

(a)

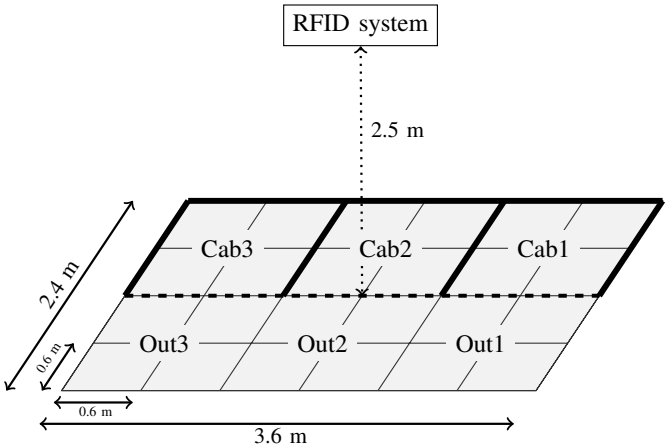

(b)

Fig. 1. (a) shows a picture of the experimental setup. The ceiling-mounted RFID system and the garments in close border proximity are highlighted. (b) depicts the dimensions and classification labels of the experimental setup.

B. Data Collection

The Impinj xArray gateway offers, amongst others, a *Wide Area Monitoring* (WAM) mode and a *Location* (LOC) mode [23]. In the WAM mode the system provides information about every read event (e.g., timestamp, RSSI, Antenna ID). The LOC mode, in contrast, estimates physical coordinates of tags within reading range of the antennas. While only the WAM mode provides the low-level RFID data we need for our approach, we also conducted the same tests in the LOC mode. We use the LOC mode data to benchmark our approach against the internal localization mode of the Impinj xArray gateway.

We collected large data sets for (i) training of the ANN model and (ii) evaluation of our approach. Both data sets were gathered in an experimental setting as shown in Fig. 1. The data for the first set were, however, collected in a different laboratory to ensure generalizability of our results. The first data set consists of two minutes of low-level RFID data for every grid field and three different numbers of tagged garments (one, two, and five items). During each of the tests, an individual stood in the experimental setup and held the garments such that they were positioned right above one of the grid fields. The garments were continuously moved up and down to reflect real-life shopping situations. The resulting data set comprises 789,631 individual tag reads.

For the evaluation of our approach we conducted 28 test cases depicting typical behavior in fitting room areas. These include combinations of seven distinct customer movement paths, different numbers of people (one and three), and different numbers of RFID-tagged objects (one, three, and nine). Each test lasted 30 seconds and was performed ten times. These 30 seconds comprise, for example, test cases with people going into one of the cabins and trying on selected garments. Garments in fitting rooms that were not tried on were put on coat hooks attached to the fitting room walls. The second data set contains 1,050,630 individual tag reads.

C. Data Preparation and ANN Instantiation

Classifying RFID-tagged objects in real-time necessitates real-time processing of RFID data streams. For this, we use a sliding window approach with windows that contain only detections from one RFID-tagged object and one collection cycle covering all 52 successively activated antenna beams. The durations of the physical cycles depend on the number of tags in the reading range of the antennas and comprise data streams ranging from one to six seconds. Despite the varying cycle durations, shifts of arbitrary length between the windows are possible (which may result in overlapping windows). We choose to evaluate our model every second to ensure regular and frequent object location updates. Class labels (i.e., *Cab1*, *Cab2*, *Cab3*, *Out1*, *Out2*, and *Out3*) are mapped to the windows based on the time they spend in the respective class. Splitting the data sets into windows results in 26,188 windows for instantiation of the ANN model and 42,446 windows for the evaluation of our approach.

Following Hauser et al. [24], we aggregate the window's low-level data and derive features that facilitate distinguishing between tags in different areas. These features are appropriately specific to RFID and must be developed based on knowledge of the particular process and the RFID hardware (e.g., number of antennas). Similar to the authors we furthermore measure the relative value of individual features in terms of classification performance. In the end, we selected 157 features. The first feature is the number of different RFID tags in the reading range of the antennas. To determine the other 156 features, we zoom in on the individual antenna level and derive values for the detections of the particular RFID tag of the antennas. We consider (i) the number of reads, (ii) the median RSSI measurement, and (iii) the maximum RSSI measurement of individual antennas.

We performed tests with ANNs with different numbers of hidden layers and nodes and in the end choose an architecture with two hidden layers and in each case 50 hidden nodes.

D. HMM modelling

We use Equation 1 to transform the output of the ANN into the HMM emission probabilities. As we do not have strong beliefs about the distribution of $P(q_n)$, we use a discrete uniform distribution as an uninformative prior.

In addition, we determine initial and transition probabilities based on our information about physical constraints and process knowledge. In the case of the initial probabilities, we assume high values for positions that are accessible from outside of the experimental setting. For the transition probabilities, we determine low values for unlikely transitions such as paths from one side of a wall to another as well as transitions over long distances within short time intervals. High probabilities, on the other hand, are determined for changes of locations that are in close proximity to each other and not affected by physical or process related barriers.

E. Performance Measures

The results of a multiclass classification problem with N classes can be summarized in the form of a confusion matrix as depicted in Fig.2.

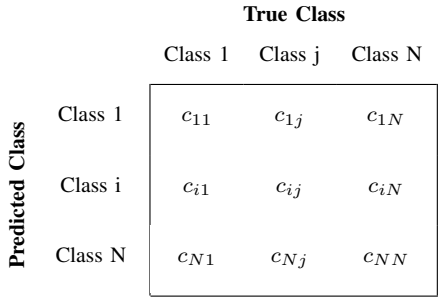

Fig. 2. Schematic multiclass confusion matrix for N classes.

The data set we use for the evaluation of our multiclass classification problem is highly imbalanced with evaluation windows that represent locations of RFID-tagged objects outside of the fitting room representing the majority class by an approximate factor of 2. To cope with this effect, we define the Class Balanced Accuracy [25]:

$$CBA_i = \frac{c_{ii}}{max(\sum_j^N c_{ij}, \sum_i^N c_{ij})} \quad (8)$$

Here, information on the number of correctly predicted cases, contained in the diagonal elements, is normalized by either the total number of observations predicted to the class (i.e., precision or positive predicted value) or the actual number of observations in that class (i.e., recall or sensitivity), decided by the greater of the two. Recall (Equation 9), on the one hand, measures the proportion of objects within true classes that is correctly predicted. Precision (Equation 10), on the other hand, measures if the predicted classes are correctly assigned to the true classes. We choose CBA as our primary measure because in case of our application precision and recall are both important for the evaluation of the performance.

$$Recall_i = \frac{c_{ij}}{\sum_i^N c_{ij}} \quad (9)$$

$$Precision_i = \frac{c_{ij}}{\sum_j^N c_{ij}} \quad (10)$$

F. Evaluation

This section starts with an overview of the classification results and then dives into a more detailed analysis by focusing on objects that are close to the border of adjacent areas (i.e., objects that hang on coat hooks attached to partition walls of adjacent cabins).

Table I shows the evaluation results for the different classes[3] and the different methods considered.

TABLE I
CLASSIFICATION RESULTS GROUPED BY CLASS. THE CBA REPRESENTS THE MINIMUM OF EITHER RECALL OR PRECISION.

Class	Method	CBA	Recall	Precision
Out	Location Mode	0.83	0.98	0.83
	Artificial NN	0.95	0.97	0.95
	Viterbi adjusted	0.95	0.98	0.95
Cab1	Location Mode	0.86	0.86	0.95
	Artificial NN	0.83	0.83	0.98
	Viterbi adjusted	0.91	0.91	0.99
Cab2	Location Mode	0.60	0.60	0.93
	Artificial NN	0.79	0.79	0.86
	Viterbi adjusted	0.95	0.97	0.95
Cab3	Location Mode	0.74	0.87	0.74
	Artificial NN	0.79	0.97	0.79
	Viterbi adjusted	0.95	0.95	0.95
All*	Location Mode	0.76	0.83	0.86
	Artificial NN	0.84	0.89	0.90
	Viterbi adjusted	0.94	0.95	0.96

*This class summarizes the results as arithmetic means of the resp. classes.

The results are based on the LOC mode's estimated physical coordinates (mapped into corresponding classes), the most probable classes estimated by the ANN, and the predicted states that we obtained by means of our adjusted Viterbi algorithm based on the same ANN predictions. We consider the results of the LOC mode as baseline of the evaluation. With 0.94 CBA, 0.95 recall, and 0.96 precision the adjusted Viterbi algorithm achieves a better overall level of classification performance than the other methods. Moreover, the overall results solely based on the ANN are also consistently better than the LOC mode's.

An analysis on class-level reveals a similar pattern. Again, the LOC mode performs generally worse. At the same time, the differences in performance of the ANN and the adjusted Viterbi require further analysis. While the performance level is comparably high for the class *Out*, the levels of the other classes differ considerably. The adjusted Viterbi consistently achieves CBAs above 0.90. In contrast, the ANN achieves 0.83 for *Cab1* and 0.79 for *Cab2* as well as *Cab3* caused by either low recall or low precision values or both.

A closer look at the confusion matrices in Fig. 3 explains the ANN's low recall and precision values for the cabins.

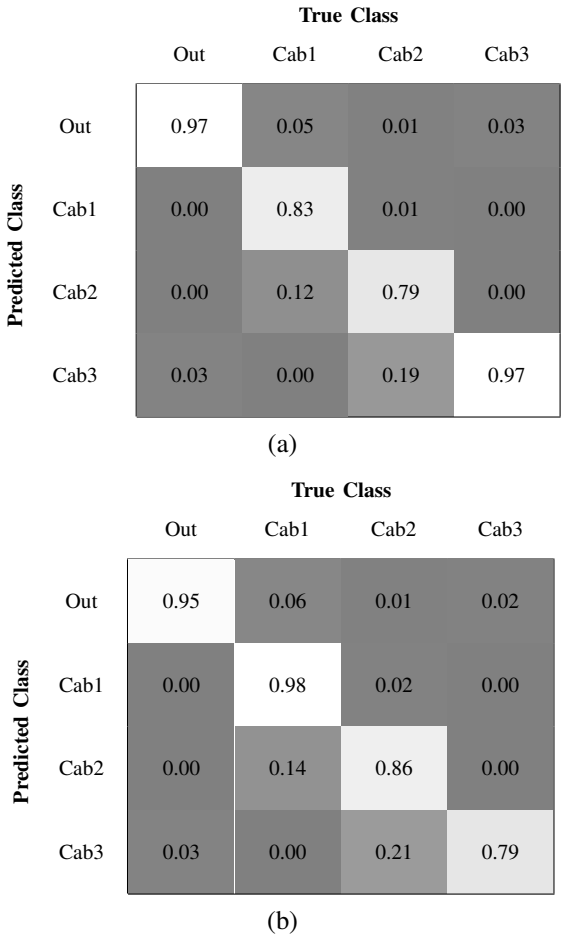

Fig. 3. Normalized confusion matrices of the ANN results. The diagonal elements show (a) the Recall values (normalized by column) and (b) the Precision values (normalized by row).

Fig. 3a shows that the recall of *Cab1* is adversely affected as 12% of the items with the true class *Cab1* are falsely

[3]We map the classes *Out1*, *Out2*, and *Out3* to the meta-class *Out* as we can not label the test data accordingly (no light barrier between the areas) and the distinction between these areas is not relevant for the use case.

assigned to *Cab2*. Similarly, 19% of the items with the true class *Cab2* are falsely assigned to *Cab3*. In exchange, the precision (Fig. 3b) of *Cab2* decreases because 14% of the items with the predicted class *Cab2* are falsely assigned to *Cab1*. Accordingly, 21% of the items with the predicted class *Cab3* are falsely assigned to *Cab2*. A possible explanation for these results can be given by the experimental setup and the test runs. As highlighted in Fig. 1a the coat hook of *Cab1* (*Cab2*) is attached to the wall adjacent to *Cab2* (*Cab3*). During the test runs, the garments that were not tried on were hung on these coat hooks and hence in close border proximity (with a maximum distance of 5 cm to the adjacent area).

For further analysis (Fig. 4), we divided the test set into subsets with (i) tags located in close border proximity and (ii) other tags (further referred to as *central*).

The LOC mode as well as the ANN are obviously not able to distinguish between areas with tags in close border proximity as the results are only slightly better than 50%. In contrast, the performance of the adjusted Viterbi for tags in close border proximity is almost as good as for central tags.

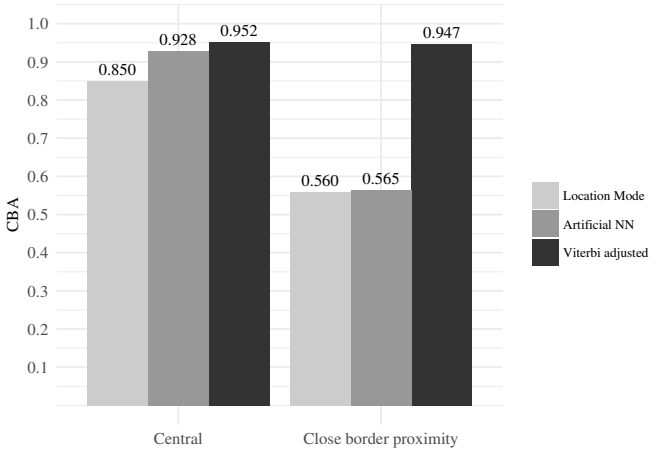

Fig. 4. CBA results of the different methods for subsets with tags located in close border proximity and others (central).

V. Conclusion

In the present paper, we propose a hybrid approach based on a HMM and an ANN to distinguish between objects in selected areas. The HMM's emission probabilities are derived from the output of an ANN model. Initial and transition probabilities of the HMM, on the other hand, are based on information about physical constraints and process knowledge. The HMM thus allows us to incorporate the dynamics of the scene.

We experimentally demonstrate the performance of our approach considering a RFID-based *smart* fitting room which represents an application with limited process control within an environment with strong multipath reflections and non-line-of-sight effects. Our results show that our approach is able to reliably distinguish between tagged objects within different cabins, including objects that hang on coat hooks that are attached to partition walls of adjacent cabins (with a maximum distance of 5 cm to the adjacent area).

To get a first glimpse of the dynamic capabilities of our approach, we implemented a prototypical real-time system [26]. The current computation time for assigning a tag to a cabin is less than a second. In accordance with the evaluation results presented in this paper, the prevailing majority of garments is correctly assigned, even in difficult cases, e.g., when customers switch cabins.

In light of our findings, we can identify opportunities for further research in various directions. First, even though our training and test sets were collected in different environments, we want to expand our tests and consider different fitting room layouts to demonstrate generalizability of our approach. Second, we want ensure feasibility under real-world conditions in actual retail stores. In addition, we see potential for incorporating more detailed process information (e.g., average time customers spend in fitting room cabins) to better estimate the parameters of the HMM.

Acknowledgment

This research was carried out under the Research Project SERAMIS (Sensor-Enabled Real-World Awareness for Management Information Systems), funded by the EU under the VII Framework Research Program.

References

[1] A. Papapostolou and H. Chaouchi, "RFID-assisted indoor localization and the impact of interference on its performance," *Journal of Network and Computer Applications*, vol. 34, no. 3, pp. 902–913, 2011.

[2] H. Liu, H. Darabi, P. Banerjee, and J. Liu, "Survey of Wireless Indoor Positioning Techniques and Systems," *IEEE Transactions on Systems, Man, and Cybernetics, Part C (Applications and Reviews)*, vol. 37, no. 6, pp. 1067–1080, Nov. 2007.

[3] M. Goller and M. Brandner, "Experimental evaluation of RFID gate concepts," in *2011 IEEE International Conference on RFID*. IEEE, 2011, pp. 26–31.

[4] D. Uckelmann and G. Romagnoli, "RF-based Locating of Mobile Objects," in *Proceedings of the 6th International Conference on the Internet of Things*. ACM, 2016, pp. 147–154.

[5] M. K. Hoang, S. Schmitz, C. Drueke, D. H. T. Vu, J. Schmalenstroeer, and R. Haeb-Umbach, "Server based indoor navigation using RSSI and inertial sensor information," in *Positioning Navigation and Communication (WPNC), 2013 10th Workshop On*. IEEE, 2013, pp. 1–6.

[6] J. Seitz, T. Vaupel, S. Meyer, J. G. Boronat, and J. Thielecke, "A hidden markov model for pedestrian navigation," in *Positioning Navigation and Communication (WPNC), 2010 7th Workshop On*. IEEE, 2010, pp. 120–127.

[7] D. Yuanfeng, Y. Dongkai, Y. Huilin, and X. Chundi, "Flexible indoor localization and tracking system based on mobile phone," *Journal of Network and Computer Applications*, vol. 69, pp. 107–116, 2016.

[8] M. Brunato and R. Battiti, "Statistical learning theory for location fingerprinting in wireless LANs," *Computer Networks*, vol. 47, no. 6, pp. 825–845, 2005.

[9] F. Thiesse, J. Al-Kassab, and E. Fleisch, "Understanding the Value of Integrated RFID Systems: A Case Study from Apparel Retail," *European Journal of Information Systems*, vol. 18, no. 6, pp. S. 592–614, Oct. 2009.

[10] P. V. Nikitin, R. Martinez, S. Ramamurthy, H. Leland, G. Spiess, and K. Rao, "Phase based spatial identification of UHF RFID tags," in *2010 IEEE International Conference on RFID (IEEE RFID 2010)*. IEEE, 2010, pp. 102–109.

[11] M. Goller, C. Feichtenhofer, and A. Pinz, "Fusing RFID and computer vision for probabilistic tag localization," in *2014 IEEE International Conference on RFID (IEEE RFID)*. IEEE, 2014, pp. 89–96.

[12] G. Li, D. Arnitz, R. Ebelt, U. Muehlmann, K. Witrisal, and M. Vossiek, "Bandwidth dependence of CW ranging to UHF RFID tags in severe multipath environments," in *2011 IEEE International Conference on RFID*. IEEE, 2011, pp. 19–25.

[13] P. Bahl and V. N. Padmanabhan, "RADAR: An in-building RF-based user location and tracking system," in *INFOCOM 2000. Nineteenth Annual Joint Conference of the IEEE Computer and Communications Societies. Proceedings. IEEE*, vol. 2. Ieee, 2000, pp. 775–784.

[14] P. Bahl, V. N. Padmanabhan, and A. Balachandran, "Enhancements to the RADAR user location and tracking system," technical report, Microsoft Research, Tech. Rep., 2000.

[15] H. Bourlard and C. Wellekens, "Links between Markov models and multilayer perceptrons," *Pattern Analysis and Machine Intelligence, IEEE Transactions on*, vol. 12, no. 12, pp. 1167–1178, Dec. 1990.

[16] M. D. Richard and R. P. Lippmann, "Neural Network Classifiers Estimate Bayesian a posteriori Probabilities," *Neural Computation*, vol. 3, no. 4, pp. 461–483, Dec. 1991.

[17] H. A. Bourlard and N. Morgan, *Connectionist Speech Recognition: A Hybrid Approach*. Springer Science & Business Media, 1994, vol. 247.

[18] H. Bourlard and N. Morgan, "Hybrid HMM/ANN systems for speech recognition: Overview and new research directions," in *Adaptive Processing of Sequences and Data Structures*. Springer, 1998, pp. 389–417.

[19] K. Murphy, *Machine Learning a Probabilistic Perspective*. Cambridge, Mass: MIT Press, 2012.

[20] A. Viterbi, "Error bounds for convolutional codes and an asymptotically optimum decoding algorithm," *IEEE Transactions on Information Theory*, vol. 13, no. 2, pp. 260–269, Apr. 1967.

[21] G. Forney, "The viterbi algorithm," *Proceedings of the IEEE*, vol. 61, no. 3, pp. 268–278, 1973.

[22] L. R. Rabiner, "A tutorial on hidden Markov models and selected applications in speech recognition," *Proceedings of the IEEE*, vol. 77, no. 2, pp. 257–286, Feb. 1989.

[23] Impinj Inc., "Impinj xArray Deployment Guide Version 5.4.0," 2015.

[24] M. Hauser, D. Zügner, C. M. Flath, and F. Thiesse, "Pushing the limits of RFID: Empowering RFID-based Electronic Article Surveillance with Data Analytics Techniques," in *Proceedings of the Thirty Sixth International Conference on Information Systems*, 2015.

[25] L. Mosley, "A balanced approach to the multi-class imbalance problem," Ph.D. dissertation, Iowa State University, 2013.

[26] M. Hauser, M. Griebel, J. Hanke, and F. Thiesse, "Empowering Smarter Fitting Rooms with RFID Data Analytics," in *Proceedings of the 13th International Conference on Wirtschaftsinformatik*, 2017.